

Measurement of flame temperature and soot amount for effective NO_x and PM reduction in a heavy duty diesel engine

To reduce exhaust NO_x and smoke, it is important to measure flame temperature and soot amount in combustion chamber. In diesel combustion it is effective to use the two-color method for the measurement of the flame temperature and KL factor, which is related with soot concentration. The diesel flame was directly and continuously observed from the combustion chamber at running engine condition by using a bore scope and a high-speed video camera.

The experimental single cylinder engine has 2.0-liter displacement and has the ability with up to five times of the boost pressure than the naturally aspirated engine by external super-charger. The devices of High Boost, Wide Range and High EGR rate at keeping a relatively high excess air ratio were installed in this research engine in order to reduce exhaust NO_x emission without smoke deterioration from diesel engines.

The video camera nac GX-1 was used in this study. From observed data under the changing EGR rates, the flame temperature and KL factor were obtained by the software of two-color method analysis. The diesel combustion processes are understood well by analyzing high-speed movies of the diesel flame motion and its temperature. The NO_x and smoke are mutually related to maximum flame temperature and also it is possible to reduce simultaneously both NO_x and soot emissions by high EGR rate in a single cylinder diesel engine.

Key words: Diesel engine, exhaust emissions, NO_x, PM, EGR, BSFC, flame temperature, two-color method, video camera

1. Introduction

Today, as future power train of passenger cars EV (Electric Vehicle), FCV (Fuel Cell V), PHV (Plug in Hybrid V) and HV (Hybrid Vehicle) are researched and developed. However, the diesel engines are commonly used as power sources for ships, railcars, trucks, buses, passenger cars and other vehicles because they are superior to other engines in terms of fuel economy, durability, and reliability. They have shown improved exhaust emissions and thermal efficiency through high pressure injection [1–4], high boost with a turbocharging and intercooler [5–8], and enhanced EGR [9, 11]. Their high thermal efficiency can suppress CO₂ emissions and many passenger cars employ diesel engines in Europe. In spite of their many advantages, the reduction of exhaust emissions and exhaust PM are strongly desired [11–13]. Especially, these reductions are needed not only in regulation but also in real world [13].

The diesel combustion consists of fuel injection into the high pressure and high temperature of compressed air and thereby it is forming and burning an air-fuel mixture instantly in combustion chamber. For this reason, the diesel combustion yields a high flame temperature in the vicinity of spray and at the core of spray a flame temperature is low because of a lack of air. Much NO_x is yielded in the vicinity of spray and in high flame temperatures. On the contrary the smoke is yielded at spray core and here is relatively low flame temperature and fuel rich. To resolve these phenomena, the flame temperature measurements have been made using flame observations by high speed camera and an analysis by a two-color method [14–25].

In this paper author measures flame temperatures and KL factor, which is closely related with soot amount, on the cases of changing EGR rates and changing fuel injection pressures and studies not only the relation between the flame temperature and BSNO_x but also the relation between soot concentration and KL factor. K means a soot

concentration and L means an optical length. Now it is difficult to separate K and L.

2. History of temperature measurement

2.1. Shift to digital image data from color film

The author studied a flame temperature and KL factor by the two-color method since 1970s [14] and showed a good relation not only between a flame temperature and an amount of NO but also between the amount of soot and KL factor by gas sampling [15]. Figure 1 shows the one of the gas sampling result and flame temperature T (dashed line).

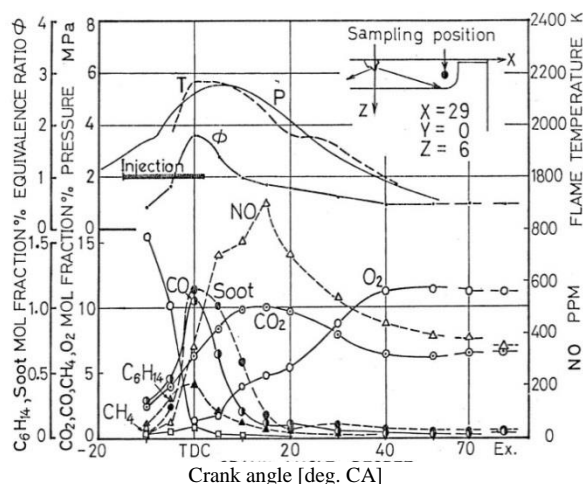


Fig. 1. Gas sampling results in comparison with flame temperature

Ahn [16] demonstrated the flame temperature measurement procedure using the two-color method with color film images of the diesel flame. The conventional mechanical high-speed film cameras have been replaced by electronic high-speed digital cameras (hereinafter designated as high-speed digital cameras), which can digitize and record image

data. The diesel flame temperature can be estimated from digital data obtained with a high-speed digital camera using the two-color method with a personal computer (PC) [17].

The temperature measurement from digital flame image by using the two-color method with a PC enables us to display easily a flame temperature distribution in a combustion chamber that had conventionally required complicated procedures to estimate by a film, and a KL factor distribution related to a smoke amount. This method contributes to NO_x and smoke reduction in exhaust emissions of a diesel engine.

2.2. Combustion observation

Conventional observation methods of diesel flame have used a combustion chamber with a large quartz observation window. These methods include the lower observation method by which a piston bottom is observed from the lower part of a combustion chamber with tempered quartz glass were conducted [18, 19]. Figure 2 shows the example of combustion photo. The upper observation method by which observation is conducted from the upper part of a cylinder head [20], and the side observation method by which or head [21, 22].

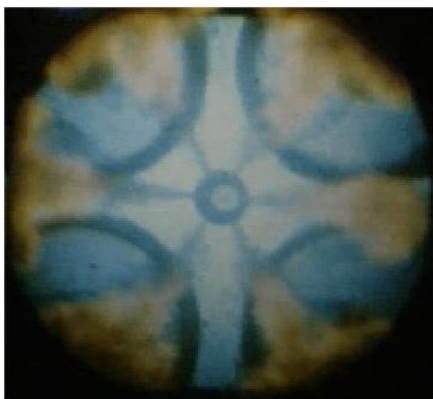


Fig. 2. Combustion photo by the lower window observation

Novel techniques included with the borescope method (by AVL proposal) were conducted by Shiozaki et al., which is combined with flame temperature measurement by the two-color method [23].

3. Analysis for flame temperature

3.1. Borescope

The author has adopted the improved borescope method, in which a 10 mm diameter is used for an optical probe (borescope) for observation of flame movement in the combustion chamber, and a diesel flame in the combustion chamber is watched through the observation hole in cylinder head, as presented in Fig. 3 [24, 25]. The observation range (red circle) in the piston combustion chamber is a part of sprays and is shown in Fig. 4. This method requires little engine modification, uses the same valve layout as the actual condition, and employs a real piston. Consequently, a diesel flame that is almost equivalent to that of a real system is visible. Because the borescope head protrudes from the underside of the head, it requires some machining to avoid interference with the piston cavity edge.

The machined portion is too small to affect combustion and the compression ratio ($\epsilon = 16.0$).

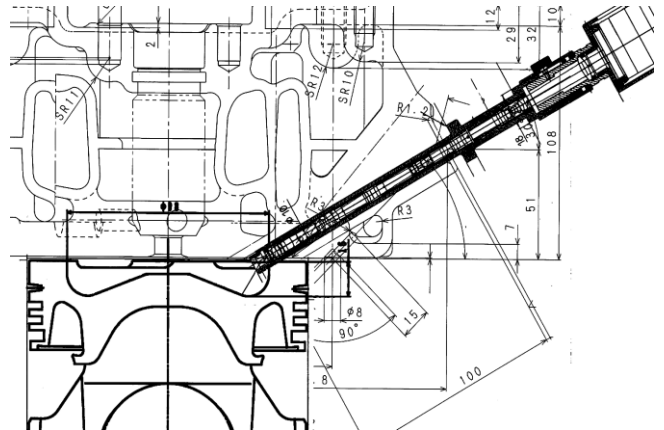


Fig. 3. Cross section of piston combustion chamber and the improved bore scope

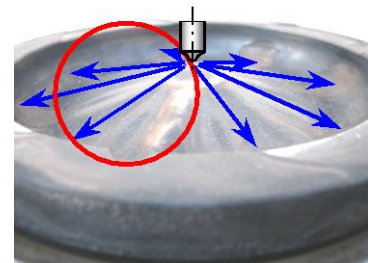


Fig. 4. Observation area in combustion chamber

In this study a high-speed digital camera (GX-1; NAC Image Technology Inc.) was used, which enables us to record images up to 200,000 fps. This study was conducted with 14,400 fps.

3.2. Two color method

Flame temperature measurements were conducted based on the diesel flame temperature analysis method using the two-color method, particularly addressing the brightness of soot particles reported by Kamimoto [14], using the flame temperature distribution analysis software developed by Tate [17] (hereinafter designated as flame temperature software).

A standard light unit for the two-color methods was used for acquiring the diesel flame temperature using flame temperature software. The calibration data for luminance and brightness temperature were shown in Fig. 5 and were



Fig. 5. Calibration data between the density and 1/T

measured by using this standard light unit. The absolute temperature scale was adopted for these calibration data in this report. The distribution of the diesel flame temperature and KL factor was obtained from the diesel flame images using the flame temperature software.

The representative value of flame temperature T_b is the average of temperatures at pixels where a flame is observed in the whole range of view. As reference Fig. 6 shows a spectral response of digital camera [17]. In this study the colors of red (610 nm) and blue (480 nm) were chosen.

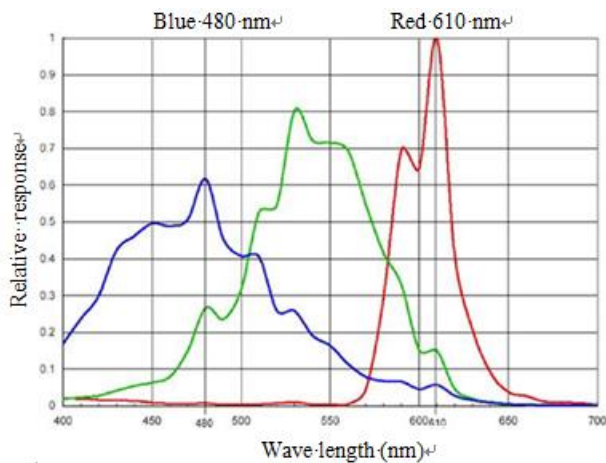


Fig. 6. Spectral response of digital camera between wave length (nm) and relative response

4. Experiment

4.1. Single cylinder test engine and system

This experiment employs a direct fuel injection diesel engine in a single-cylinder and four stroke cycle with boost pressure up to 600 kPa is applicable with an external motor-driven supercharger [9]. Figure 7 presents a system diagram of the research single-cylinder engine. It has a common rail injection system with fuel injection pressure up to 220 MPa, a mini sac nozzle, a nozzle hole diameter of 0.177 mm, eight nozzle holes, and a nozzle hole angle of 150°. The swirl ratio R_s generated from a cylinder head port was set constant as 1.4. A steel monotherm piston was used, for which the cross sectional view is presented in Fig. 3. Table 1 presents specifications of the single cylinder research engine.

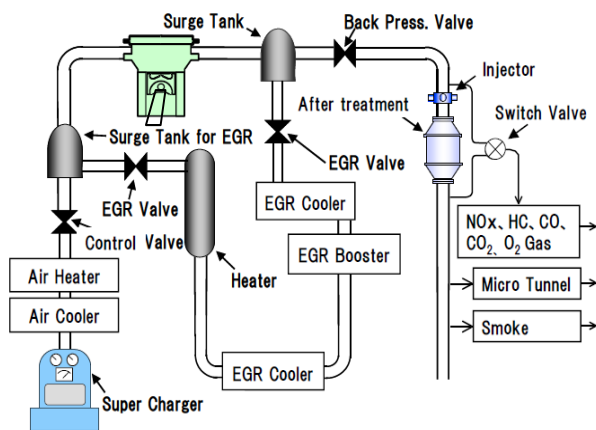


Fig. 7. Schema of experimental apparatus

Table 1. Engine specifications

Item	Specifications
Engine type	DI single cyl., 4 Valve
Displacement	2.004 L
Bore × stroke	135×140 mm
Max engine speed	2000 rpm
Injector	Common Rail system (Max Pinj = 220MPa)
Nozzle	Minisac φ 0.177×8-150°
Piston type	Steel piston (monotherm)
Comb. chamber	Toroidal (φ98 mm)
Compression ratio	16.0
Swirl ratio	1.4
Valve actuation	Cam-less VVA
Air charging system	External super charger

Table 2. Fuel properties for the test

Category	Properties	Category	Properties	
Density 15°C	g/cm ³ 0.8268	Elements mass %	C 86.1	
Kinematic	mm ² /s 3.978		H 13.8	
Viscosity 30°C			O —	
Flash Point	°C 69.0		N <0.1	
Cetane Index (JIS K2280)	61.0	Components vol %	Saturates 83.4	
Cetane Number	57.1		Olefins 0.0	
			Aromatics 16.6	
Distillation °C	IBP	175.5	Mono-	15.4
	5%	205.5	Di-	1.0
	10%	222.5	+Tri-	0.2
	50%	286.5	Calorific Value	kJ/kg 45900
	90%	332.5	Lower Calorific Value	kJ/kg 43030
EP	354.5			
Sulfur	mass ppm 6	HFRR (WS1.4)	μm 233	

4.2. Experimental conditions and variables

Experimental conditions are described as follows. Boost pressure $P_b = 271.3$ kPa and head swirl ratio $R_s = 1.4$ were fixed as common, and fuel injection pressure $P_{inj} = 200$ MPa and EGR rate = 50% were set as the standard conditions at engine speed $N_e = 1,200$ rpm. The brake mean effective pressure $BMEP = 1.0$ MPa (indicating a mean effective pressure $IMEP = 1.2$ MPa around), and fuel amount a stroke was $q = 135$ mm³/st. The following factors were varied.

The EGR rate was determined from the measurement of intake CO_2 concentration when exhaust CO_2 was mixed with the intake.

- The EGR rate was varied as 0, 30, 50, and 55% with the fuel injection pressure (Common-rail pressure) P_{inj} was fixed constant as 200 MPa.
- Fuel injection pressure P_{inj} was varied as 90, 150, 200, 220 MPa with the EGR rate fixed constant at 50%.

In the experiments the oxygen concentration of intake air containing EGR gas was measured at inside of the intake manifold, exhaust pressure was adjusted to the same pressure as the intake pressure P_b , and engine intake air temperature T_{in} was set to $50 \pm 1^\circ C$. These conditions were the same as performance and exhaust emission tests.

5. Experimental results and discussions

5.1. Exhaust emissions and BSFC by changing EGR rate and injection pressure

Figure 8, 9, and 10 respectively present changes in exhaust emissions, fuel consumption performance (BSFC), and the excess air ratio λ when the EGR rate was varied as 0, 30, 50, and 55% and the fuel injection pressure (common rail pressure) Pinj was varied as 90, 150, 200 and 220 MPa.

Figure 8 shows that BSNO_x is reduced drastically from 21 g/kWh to 0.5 g/kWh at Pinj = 220 MPa, whereas BSHC and BSCO change little at a low factor, when EGR rate is increased from 0% to 55%. Smoke tends to increase by increment in the EGR rate. It increases only at Pinj = 90 MPa in the case of EGR rate = 50%, but it shows no increase at Pinj = 150 MPa and higher. Smoke then jumps up at EGR rate = 55%, but there is a little increase in smoke at Pinj = 200 and 220 MPa. It can be effective to reduce an amount of soot and PM by high pressure injection such as 200 MPa level.

Figure 9 suggests that BSFC varies a little by the EGR rate increase, and BSFC is minimum at Pinj = 220 MPa in

the case of EGR rate = 50%. Accordingly, when the EGR rate is enhanced to 50%, the fuel consumption rate reduces a little as fuel injection pressure is raised. Although Pmax varies a little with the increase in the EGR rate, it rises as the fuel injection pressure increases. The pressure diagram changes a little because the air capacity of the cylinder is about the same even if the EGR rate is increased. However Pmax rises as the fuel injection pressure increases because the peak of rate of heat release (ROHR) shifts to earlier timing. The NO_x concentration is expressed in parts per million (ppm) and reduces gradually with increasing EGR rate.

Figure 10 shows the intake CO₂ concentration, excess air ratio λ, intake O₂ concentration, and other results at an enhanced EGR rate. The excess air ratio λ is reduced from 4 to 2 as the EGR rate increases from 0% to 50%.

5.2. Increasing EGR rate

Figure 11 shows ROHR at EGR rates = 0, 30, 50, and 55% for injection pressure Pinj = 200 MPa. The photos of combustion at each crank angle after the ignition starting period of TDC are displayed in Fig. 12.

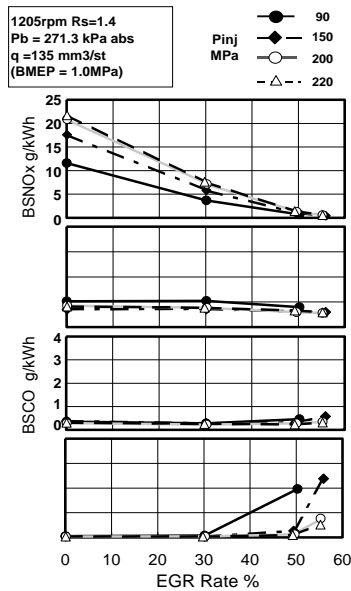


Fig. 8. Emission by changing EGR rate

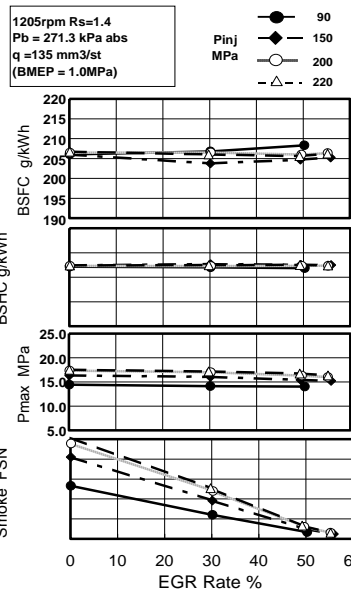


Fig. 9. Efficiencies by changing EGR rate

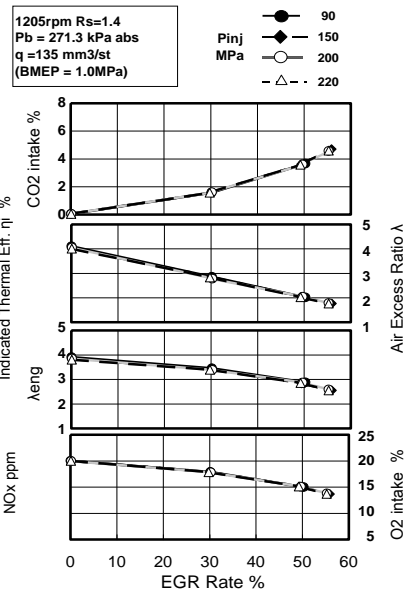


Fig. 10. Excess air ratio by changing EGR rate

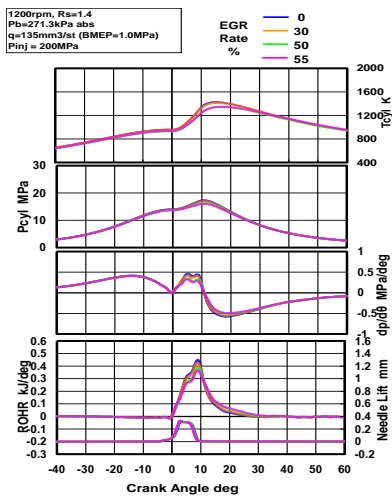


Fig. 11. ROHR by changing EGR rate

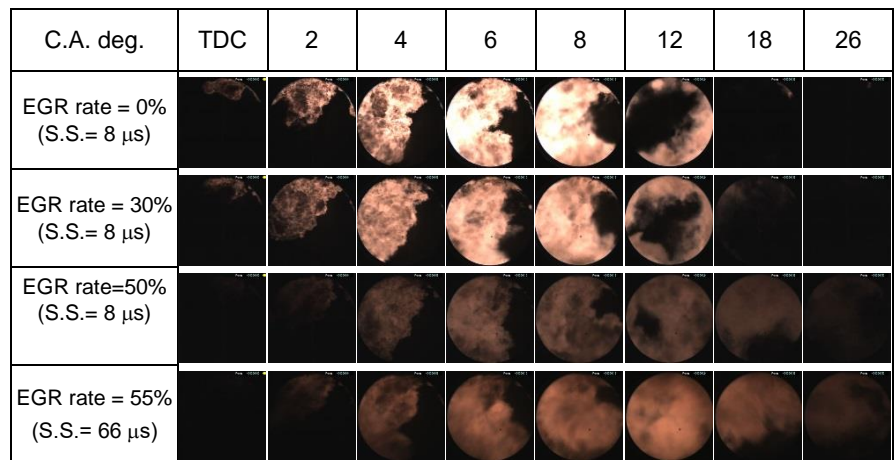


Fig. 12. High speed flame photos with borescope by changing EGR rate

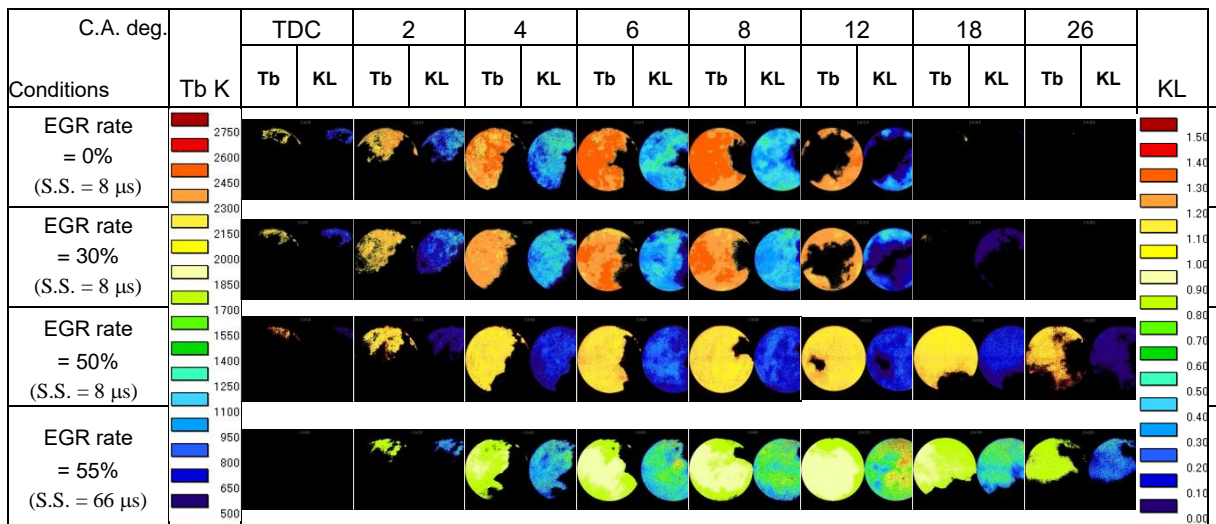


Fig. 13. Distribution images of flame temperature Tb and KL factor by changing EGR rates

The distribution of the flame temperature and KL factor to crank angle corresponding to these conditions are presented in Fig. 13, so that all EGR rate conditions from 0% to 50% can be compared. In the case of EGR rate 55% the flame temperature is low and KL factor is high in comparison with the case of EGR rate 50%. In the case of EGR rate 55% the smoke concentration (FSN) is high in exhaust pipe.

Figure 12 presents the sequential photographs of a diesel flame at each crank angle by the EGR rate increases. The flame brightness decreases significantly as the EGR rate increases, which implies that the flame temperature decreases as the EGR rate increases.

Figure 13 displays the analytical result of diesel flame at an enhanced EGR rate with the flame temperature software, flame temperature distribution, and KL factor distribution at each crank angle. The flame temperature decreases significantly as the EGR rate increases: 2500 K at EGR rate = 0%, and 1900 K at EGR rate = 55%. This flame temperature drop brings about drastic reduction of BSNO_x. The KL factor is also related to exhaust smoke because it increases at EGR rate = 55%.

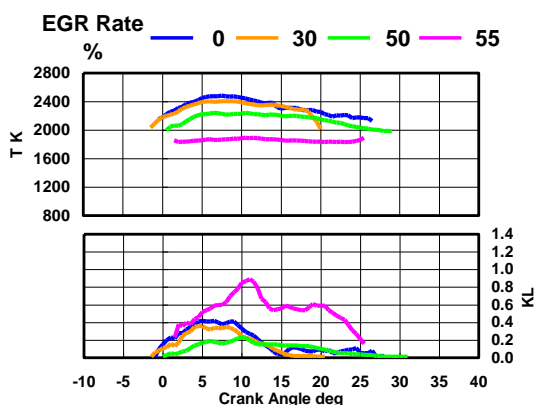


Fig. 14. Averaged Tb and KL factor by changing EGR rates

Figure 14 displays the variation of flame temperature and KL factor determined by flame images in the observation range of the borescope at each crank angle at EGR rate = 0, 30, 50, and 55%. The peak values of flame temperature

Tb vary largely from 2500 K to 1900 K by increasing EGR rate and the difference is large with 600 K. On the contrary the thermodynamic mean temperatures T_{cy1} in Fig. 11 vary a little from 1400 K to 1350 K and the difference is small with 50 K. The reason of BSNO_x reduction by increasing EGR rate can't be explained due to the decreasing of the thermodynamic mean temperature. Then it is very important to measure the flame temperature and the diesel combustion phenomenon in the cylinder should be understood for the reduction of exhaust emissions.

5.3. Increasing injection pressure

The change in ROHR as injection pressure Pinj is increased from 90 MPa to 150, 200 and 220 MPa is presented in Fig. 15 at EGR rate = 50%. Figure 16 displays the combustion photos at each crank angle from the ignition starting

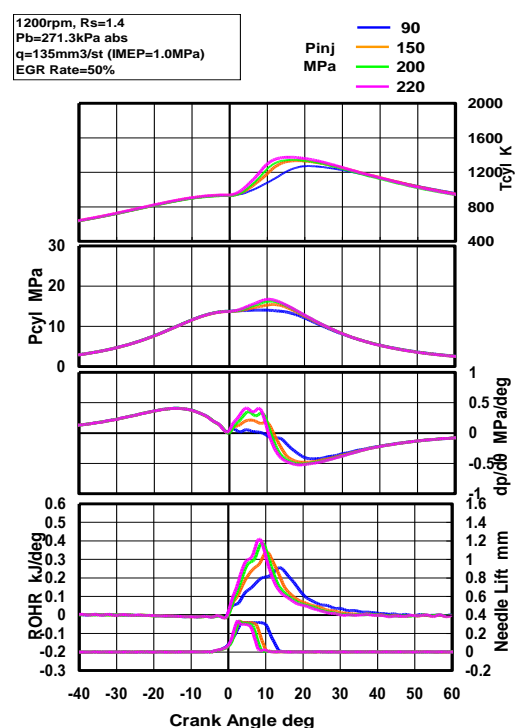


Fig. 15. ROHR by Changing Pinj at EGR rate 50%

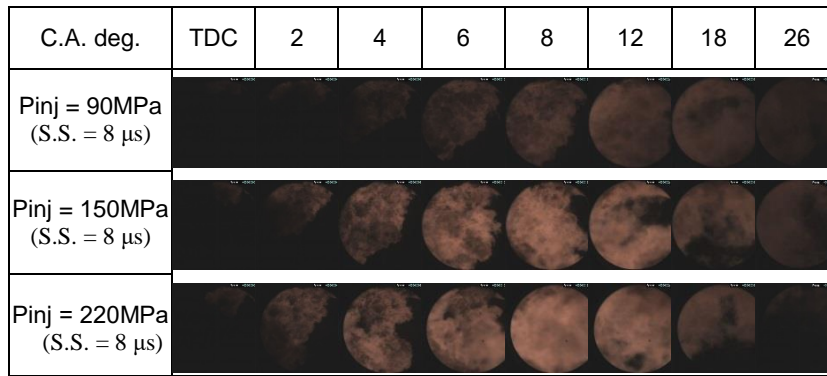


Fig. 16. High speed flame photos with borescope by changing Pinj at EGR rate 50%

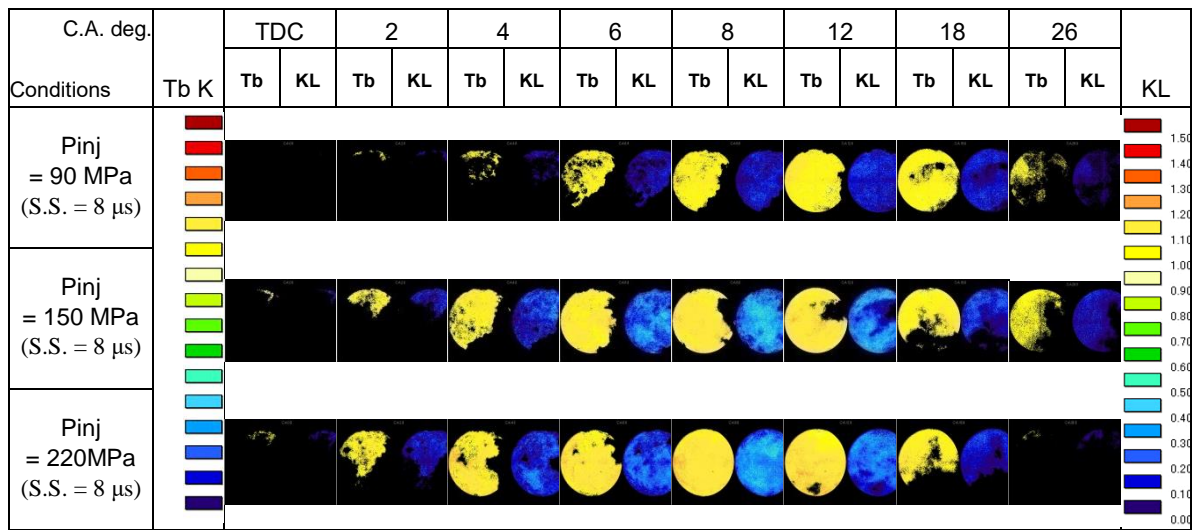


Fig. 17. Distribution images of flame temperature Tb and KL factor by changing Pinj at EGR rate 50%

period of TDC, so that conditions can be compared when Pinj = 90, 150, 200 and 220 MPa at EGR rate = 50%. The distribution of the flame temperature and KL factor are presented in Fig. 17 in the same way. Figure 18 shows their variation in reference to the crank angle. The case of Pinj = 200 MPa is abbreviated in Fig. 16 and Fig. 17 because of that is already shown in Fig. 12 and 13.

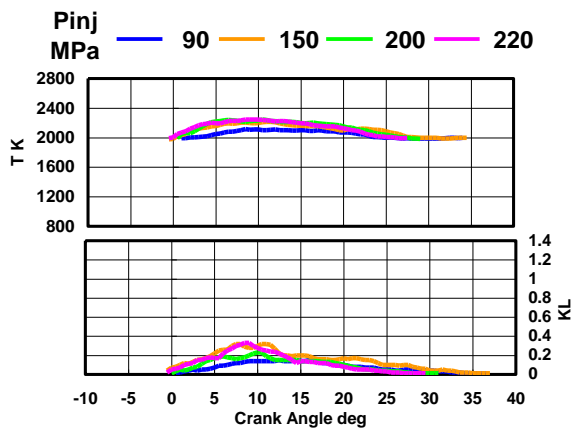


Fig. 18. Averaged Tb and KL factor by changing Pinj at EGR rate 50%

Pinj is changed from 90 MPa to 150, 200 and 220 MPa at EGR rate = 50%. Although BSNOx is already low and

smoke is high at Pinj = 90 MPa, it is necessary to raise Pinj to 150 MPa to reduce smoke. BSFC can be reduced further by increasing Pinj to 220 MPa. It is, after all, a necessary technology to combine high EGR rate and high pressure injection for reduction in exhaust emissions and fuel consumption, as widely acknowledged.

The flame photographs in Fig. 16 suggest that the brightness is low and combustion is not active at Pinj = 90 MPa, although combustion is active and brightness is high at Pinj = 150 and 220 MPa. The flame temperature at each condition of 6–12 deg. CA shows a peak of 2230 K at Pinj = 220 MPa, which is not too high temperature because the EGR rate = 50%, so that BSNOx stays low.

As the author mentioned above, it is very important to measure the flame temperature and KL factor, which is related with soot amount. By the measurement the diesel combustion phenomenon in the cylinder should be understood well for the reduction of exhaust emissions such as BSNOx, smoke and PM in a multi-cylinder engine. The author has improved successfully BSFC and exhaust emissions of a 6-cylinder heavy duty diesel engine by using high EGR rates [26].

6. Conclusion

The measurements were conducted on conditions of engine speed Ne = 1200 rpm and fuel amount of stroke q = 135 mm³/st, with a middle load where high boost engines

are frequently used on road as BMEP = 1.0 MPa around. Fuel injection pressure Pinj and the EGR rate were varied within 90–220 MPa and 0–55%, respectively.

The following results were obtained.

- It was confirmed that the diesel combustion flame temperature is measurable using the two-color method from digital data obtained with an electronic high-speed digital camera. Moreover, it was verified that diesel flame observation by the borescope system is useful. It is very important to measure the flame temperature and KL factor for the reduction of exhaust emissions.
- When the EGR rate was varied from 0% to 55% at Pinj = 200–220 MPa, BSNO_x dropped to 1/40 and the flame

temperature also fell from 2500 K to 1900 K, which corresponded well with the BSNO_x drop.

- As the fuel injection pressure was increased from 90 MPa to 220 MPa at EGR rate = 50%, the flame temperature tended to increase slightly. But Smoke decreases very largely and PM in exhaust pipe drops largely.

Acknowledgements

This study was made by annual research fund from investors in the New A.C.E. Institute Co. Ltd. The author express their deepest gratitude for the investor's kind support.

Nomenclature

BMEP: Brake mean effective pressure, MPa
 BSFC: Brake specific fuel consumption, g/kWh
 BSCO: CO weight per effective power and time, g/kWh
 BSHC: HC weight per effective power and time, g/kWh
 BSNO_x: NO_x weight per effective power and time, g/kWh
 EGR rate: EGR rate by [CO₂] at intake air, %
 IMEP: Indicated mean effective pressure, MPa
 Ne: Engine speed, rpm
 Pb: Boost pressure, kPa
 Pinj: Fuel injection pressure (at Common rail), MPa
 Pmax: Maximum or peak cylinder pressure, MPa
 Pcyl: Cylinder pressure, MPa

q: Fuel quantity per stroke, mm³/st
 ROHR: Rate of heat release, kJ/deg
 Rs: Swirl ratio, –
 Smoke: Smoke, FSN
 S.S.: Shatter speed, μs
 Tb: Flame temperature by soot, K
 Tcyl: Mean cylinder gas temperature, K
 Tin: Intake air temperature included EGR gas, C
 dP/dθ: Rate of cylinder pressure rise, kPa/deg
 λ: Excess air ratio, –
 λ eng: Engine excess air ratio considering whole [O₂], -

Bibliography

- [1] SHUNDOH, S., KAKEGAWA, T., TSUJIMURA, K., KOBAYASHI, S. a study on combustion of direct injection diesel engine with 150 MPa injection pressure. *Proceedings of International Symposium COMODIA* 90. 1990, 607-612.
- [2] WOODS, M., KAMO, R., BRYZIK, W. High pressure fuel injection for high power density diesel engines. *SAE Technical Paper* 2000-01-1186. 2000. DOI: 10.4271/2000-01-1186
- [3] ITOH, S., NAKAMURA, K. Reduction of diesel exhaust gas emission with common rail system. *Journal of JSAE*. 2001, **55**(9), 46-52.
- [4] AOYAGI, Y., KUNISHIMA, E., ASAUIMI, Y. et al. Diesel combustion and emission using high boost and high injection pressure in a single cylinder engine. *JSME International Journal, Series B*. 2005, **48**(4), 648-655.
- [5] ENDO, S., OTANI, T., KAKINAI, A. An improvement of pumping loss of high boosted diesel engines. *SAE Technical Paper* 885102. 1988. DOI: 10.4271/885102
- [6] SUGIHARA, H., NAKAGAWA, H., SHOUYAMA, K., YAMAMOTO, A. Hino New K13C diesel engine equipped with common rail type fuel injection equipment. *Engine Technology*. 1999, **1**(4), 40-45.
- [7] TSUJITA, M., NIINO, S., ISHIZUKA, T. et al. Advanced fuel economy in Hino New P11C turbocharged and charge-cooled heavy duty diesel engine. *SAE Technical Paper* 930272. 1993. DOI: 10.4271/930272
- [8] STOVER, T., REICHENBACH, D., LIFFERTH, E. The Cummins Signature 600 heavy-duty diesel engine. *SAE Technical Paper* 981035. 1998, DOI: 10.4271/981035
- [9] AOYAGI, Y., OSADA, H., MISAWA, M. et al. Advanced diesel combustion using of wide range, high boosted and cooled EGR system by single cylinder engine. *SAE Technical Paper* 2006-01-0077. 2006. DOI: 10.4271/2006-01-0077
- [10] KNECHT, W. European emission legislation of heavy duty diesel engines and strategies for compliance. *Proceedings of the Thermo-and fluid Dynamic Processes in Diesel Engines* (THIESEL 2000), 2000, 289-302.
- [11] ADACHI, T., AOYAGI, Y., KOBAYASHI, M. et al. Effective NO_x reduction in high boost, wide range and high EGR rate in a heavy duty diesel engine. *SAE Technical Paper* 2009-01-1438. 2009. DOI: 10.4271/2009-01-1438
- [12] Japan Ministry of Environment, About New Automotive Emission Standards in future (8th Report) (in Japanese), 2005.
- [13] The international council on clean transportation (icct), www.theicct.org. NO_x emissions from heavy-duty and light-duty diesel vehicles in the EU: Comparison of real-world performance and current type-approval requirement. Briefing, December 2016.

- [14] KAMIMOTO, T., MATSUOKA, S., MATSUI, Y., AOYAGI, Y. *PIME*. 1975, C96/75, 139.
- [15] AOYAGI, Y., KAMIMOTO, T., MATSUI, Y., MATSUOKA, S. A gas sampling study on the formation processes of soot and NO in a DI diesel engine. *SAE Technical Paper* 800254. 1980, DOI: 10.4271/800254
- [16] AHN, S.G., KAMIMOTO, T., MATSUI, Y., MATSUOKA, S. *Transaction of JSAE*. 1981, **47**(417), 896-903.
- [17] TATE, R. *Journal of the ILASS-Japan*. 2009, **18**(63), 103-110.
- [18] KOBAYASHI, S., SAKAI, T., NAKAHIRA, T. et al. Measurement of flame temperature distribution in D.I. diesel engine with high pressure fuel injection. *SAE Technical Paper* 920692. 1992, DOI: 10.4271/920692
- [19] AOYAGI, Y., ASAUMI, Y., KUNISHIMA, E., HARADA, A. Visualized analysis of a pre-mixed diesel combustion under the high boosting engine condition. *Proceedings of International Symposium COMODIA 2001*. 2001, 434-440.
- [20] GENZALE, C.L., REITZ, R.D., MUSCULUS, M.P.B. Effects of jet-bowl and jet-jet interactions on late-injection low-temperature heavy-duty diesel combustion. *Proceedings of the Thermo-and Fluid Dynamic Processes in Diesel Engines* (THIESEL 2008). 2008, 277-297.
- [21] KUWAHARA, K., KAWAI, T., ANDO, H. Influence of flow field structure after the distortion of tumble on lean-burn flame structure. *Proceedings of International Symposium COMODIA 94*. 1994, 89-94.
- [22] MANCARUSO, E., MEROLA, S.S., VAGLIECO, B.M. Study of the multi-injection combustion process in a transparent direct injection common rail diesel engine by means of optical techniques. *International Journal of Engine Research*. 2008, **9**(6), 483-498.
- [23] SHIOZAKI, T., MIYASHITA, A., AOYAGI, Y., JOKO, I. The analysis of combustion flame in a DI diesel engine (part 2-hydroxyl radical emission versus temperature). *Proceedings of International Symposium COMODIA 94*. 1994, 23-528.
- [24] FUJINO, R., AOYAGI, Y., OSADA, H. et al. Direct observation of clean diesel combustion using a bore scope in a single cylinder HDDE. *SAE Technical Paper* 2009-01-0645. 2009. DOI: 10.4271/2009-01-0645
- [25] AOYAGI, Y., OSADA, H., SHIMADA, K., TATE, R. High EGR rate combustion and its flame temperature observed by a bore scope system in a heavy duty diesel engine. *Proceedings of the Thermo-and fluid Dynamic Processes in Diesel Engines* (THIESEL 2012). 2012.
- [26] AOYAGI, Y. Improvement of BSFC and effective NO_x and PM reduction by high EGR rates in heavy duty diesel engine. *Combustion Engines*. 2017, **171**(4), 4-10. DOI: 10.19206/CE-2017-401

Yuzo Aoyagi, DEng. – Company friend of New A.C.E. Institute Co. Ltd., Japan.
e-mail: aoyagiyz1@jcom.zaq.ne.jp

